Effect of interlayer thickness on shear deformation behavior of AA5083 aluminum alloy/SS41 steel plates manufactured by explosive welding

JUN HYUN HAN, JAE PYOUNG AHN, MYUNG CHUL SHIN
Division of Materials Science and Technology, Korea Institute of Science and Technology, P.O. Box 131, Cheongryang, Seoul, 130-650, Korea
E-mail: jhhan@kist.re.kr

An AA5083 aluminum alloy plate and an SS41 steel plate were cladded by an explosive welding method using an AA1050 aluminum alloy interlayer plate. The effects of the interlayer thickness on the interface morphology and the shear deformation behavior of the cladded plates were studied. The interfacial zone was composed of an intermetallic compound, $FeAl_3$, formed by the AA1050 interlayer. The intermetallic compound acted as a crack source at the AA1050/SS41 interface, and the thickness and morphology of the interfacial zone were depended on the thickness of the AA1050 interlayer. In a shear deformation test, the crack propagation behavior varied according to the morphologies of the interfacial zone, and the shear strength of the cladded plates decreased with the interlayer thickness. © *2003 Kluwer Academic Publishers*

1. Introduction

The explosive welding of two different kinds of metallic plates is achieved by the intensive deformation due to high pressure and high temperature generated at the collision point. Extensive researches on explosive welding have been focused on the microstructural changes at the interface between the different kinds of metals [1–4] and the effects of base plate or flyer plate on the wave morphology in welded interfaces [5]. Most explosive welding processes have been performed without any interlayer. However, depending on the material pairs, the third material was introduced as an interlayer [6, 7]. For example, when an aluminum bush-bar in an aluminum refining factory is welded by an explosive welding method, a titanium interlayer plate is inserted between the steel and the aluminum to suppress the formation of the brittle intermediate phase which plays a deadly effect on lifetime of the cladded product. It is also very difficult to weld directly the combination of aluminum alloy and stainless steel plates. For this combination, Hokamoto *et al.* [7] used another stainless steel plate as an interlayer in welding an Al-Mg alloy and a stainless steel plate, and the interlayer lead to changes in morphologies and mechanical properties of interface.

Although the interlayer has been used to minimize a brittle interfacial zone and to improve the weldability, the study on the effects of the interlayer has still been limited. In this work, the multiplates with AA5083/AA1050(interlayer) aluminum alloys/SS41 steel sequence were manufactured by the explosive welding method, and the variations of the interface morphology and the shear properties with thickness of the AA1050 aluminum alloy interlayer were investigated.

2. Experimental procedure

Fig. 1 shows a schematic illustration of the explosive welding process. A single-shot explosion process, which is welded at one shot, was conducted to cut down cost and simplify process parameters. A 9 mm thick steel (SS41) plate and a 5 mm thick aluminum alloy (AA5083) plate were used as a base and a flyer plate, respectively. The thickness of the AA1050 aluminum alloy interlayer was varied from 0.2 to 2 mm. All the plates were polished both mechanically and chemically to obtain a clean surface before explosive welding. Explosive was packed on the flyer plate and a detonator was set on one corner of the flyer plate, as shown in Fig. 1. The chemical compositions of the AA1050, AA5083 aluminum alloys, and the SS41 steel plate are presented in Table I. The process parameters such as explosive thickness, stand-off distance, and collision angle were constant in this work. The direct welding without an interlayer plate was also conducted under the same welding condition for comparison with other specimens with an interlayer.

The microstructures of each welded interface were observed using the backscattered electron (BE) detected attached to a scanning electron microscope (SEM) and a transmission electron microscope (TEM). In particular, the phase analysis of the interfacial zone formed at the AA1050/SS41 boundary was conducted from selected area diffraction (SAD) and convergent beam electron diffraction (CBED) patterns taken by TEM.

To evaluate bond strengths at the AA5083/AA1050 and the AA1050/SS41 boundaries, a shear deformation test was performed, with the specimen designed as shown in Fig. 2, using a tensile test machine (INSTRON) at a constant crosshead speed of 1.0 mm/min. The center line of the AA1050 aluminum alloy interlayer was parallel to the longitudinal direction of the specimen, as shown in Fig. 2, and was aligned along a loading axis of the INSTRON. Thus the two welded boundaries, AA5083/AA1050 and AA1050/SS41, between the notches, were under the same shear stress. The maximum shear strength and elongation were obtained from an average of 5 shear tests per specimen. After the shear deformation test, the fractured surfaces were investigated by the BE image mode. An area fraction of each phase on the fractured surfaces was analyzed using Image-Pro 4.01 software.

TABLE I Chemical compositions of AA5083, SS41, and AA1050 used as flyer, base, and interlayer plate, respectively

	Chemical composition (wt%)					
	Fe	Si	Mn	Mg	Cr	Al
AA1050	0.24	0.12	<0.01			bal.
AA5083			0.9	4.5	0.15	bal.
	C	Si	Mn	Fe		
SS41	0.12	0.27	0.72	bal.		

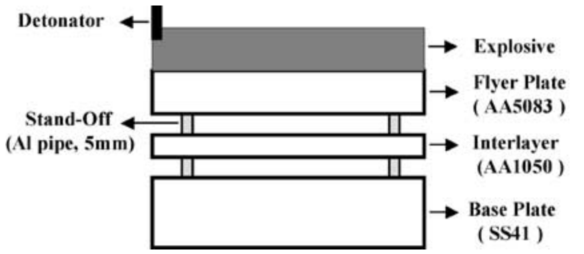

Figure 1 Schematic illustration of explosive welding.

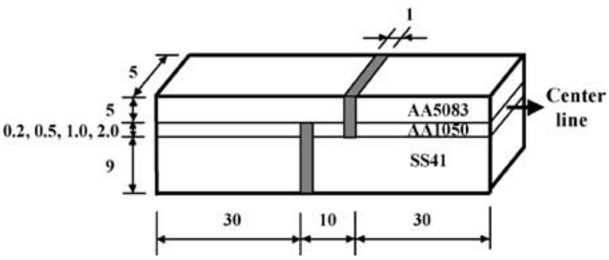

Figure 2 The shape and dimensions (in mm) of shear deformation test specimen.

3. Results and discussion

3.1. Microstructure of welded interface

The direct-welded AA5083 aluminum alloy/SS41 steel plate without the AA1050 aluminum alloy interlayer had so weak a bond strength that separation at the interface took place during the flattening of the as-welded plate. From this result, it was confirmed that it was very difficult to weld the AA5083 aluminum alloy plate and SS41 steel plate without a soft interlayer. In most cases of explosive welding, the wavy shapes of the interface were formed due to a fluid-like behavior of the materials under high pressure and high strain rate. In this study, interfaces with shapes different from the wavy shape were formed, as shown in Fig. 3, depending on the thickness of AA1050 interlayer plate. The interface shape of AA5083/AA1050 pair appeared almost straight, irrespective of the interlayer thickness. On the other hand, a new layer (interfacial zone) was formed at the AA1050/SS41 boundary, as indicated by arrows in Fig. 3, and irregular wavy interfaces were found between the interfacial zone and base plate (SS41). The interfacial zone could be formed at high temperature due

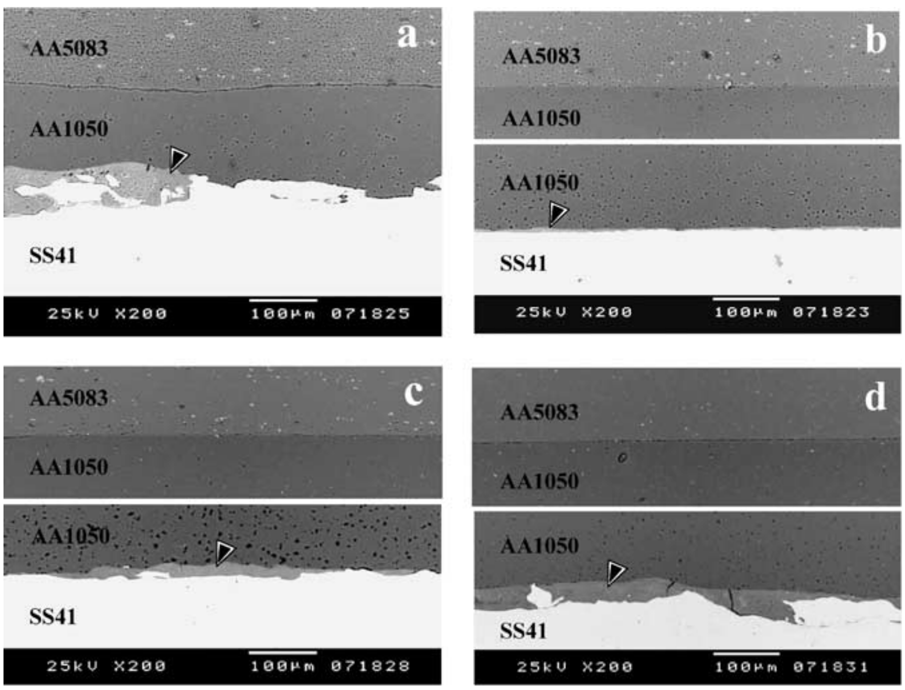

Figure 3 Backscattered electron (BE) images of the specimens explosively welded using the interlayer thickness of (a) 0.2 mm, (b) 0.5 mm, (c) 1.0 mm and (d) 2.0 mm. The arrows indicate interfacial zone formed and two images showing upper and lower interface are shown together in (b), (c), and (d).

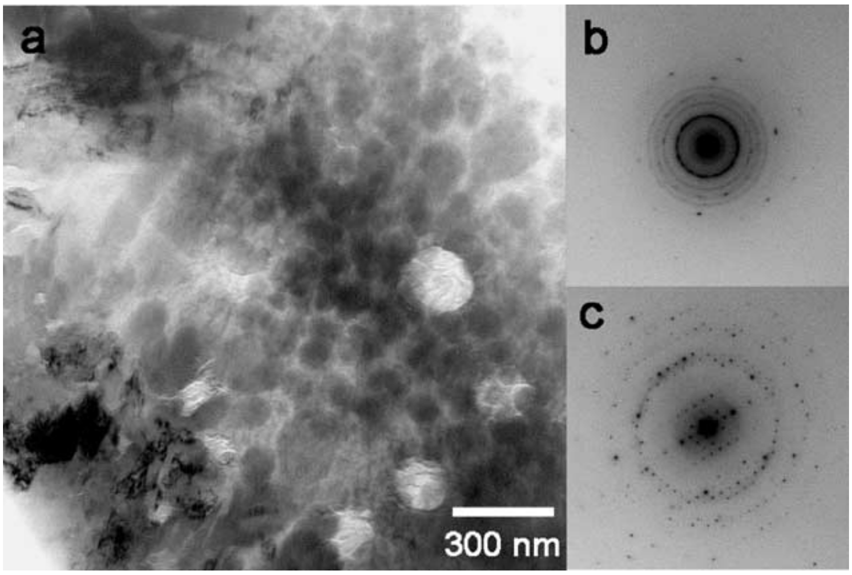

Figure 4 (a) Bright field image of interfacial zone, (b) selected area diffraction (SAD) pattern, and (c) convergent beam electron diffraction (CBED) pattern taken by transmission electron microscope.

to the collision energy resulting from explosion. However, the morphological changing mechanism in formation of the interfacial zone has not clearly known yet.

A uniform interfacial zone was observed at the interface of all specimens, except the specimen with the 0.2 mm-thick interlayer (Fig. 3a), in which it was found to be discontinuous but only at the front vortex area of the interface. On the other hand, the thickness of the interfacial zone increased with interlayer thickness as shown in Fig. 3b, c and d. This was attributed to the fact that the loss of kinetic energy from the collision was proportionate to interlayer thickness [7]. Internal cracks were appeared in the interfacial zone, as shown in Fig. 3, and were attributed to the combination of the brittle nature of the interfacial zone itself and the difference in the thermal expansion coefficient of the materials at the interfacial zone/SS41 boundary or the AA1050/interfacial zone boundary.

Detailed observations and phase analysis in the interfacial zone were conducted by TEM, and Fig. 4 shows (a) a bright field image, (b) SAD pattern, and (c) CBED pattern of the specimen with interlayer thickness of 1 mm. The interfacial zone was composed of nano-sized grains. From SAD and CBED patterns obtained from a grain among the nanocrystal grains, the nano-sized grains were confirmed to be an intermetallic compound with a crystal structure of $FeAl_3$, which had the zone axis of $\langle 112 \rangle$ and the cell volume of $1401.3 Å^3$. Therefore, the AA1050 interlayer lead to the formation of an interfacial zone composed of $FeAl_3$ intermetallic compounds at AA1050/SS41 boundary, and the thickness and morphology of the interfacial zone was depended on the interlayer thickness.

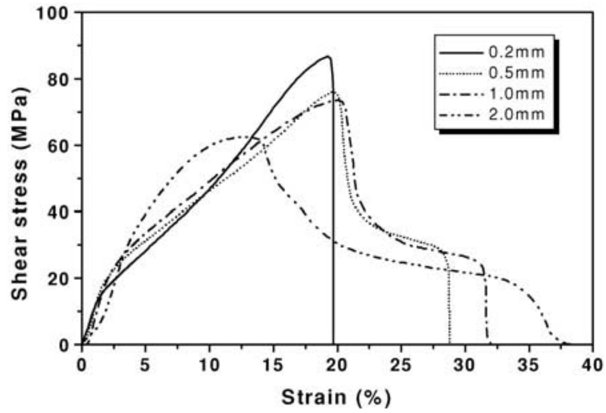

Figure 5 The engineering shear stress and strain curves showing the deformation behavior of welded specimens with interlayer thickness during shear test.

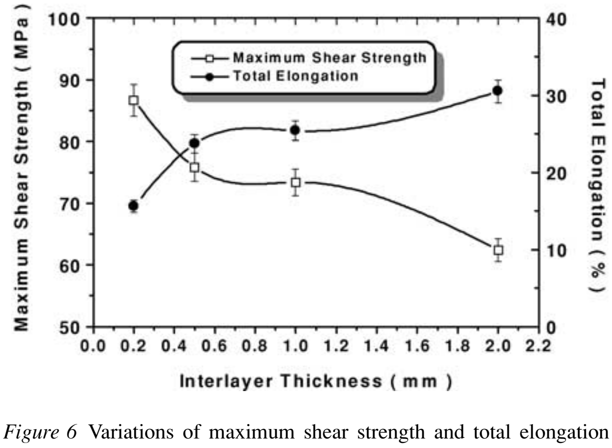

Figure 6 Variations of maximum shear strength and total elongation with interlayer thickness.

3.2. Shear deformation and fractographic analysis

The engineering shear stress and strain curves of the welded specimens in Fig. 5 show the variation of the deformation behavior with interlayer thickness during the shear test. Fig. 6 also shows the variation of maximum shear strength and elongation with interlayer thickness. The specimen with interlayer of the thinnest thickness (0.2 mm) showed the highest shear strength, which was due to the second hardening, that indicates the extra hardening appeared after the normal work hardening in the plastic deformation region of the stress-strain curve. This implies that some welded interface with a stronger bond strength was acted as other routes for crack

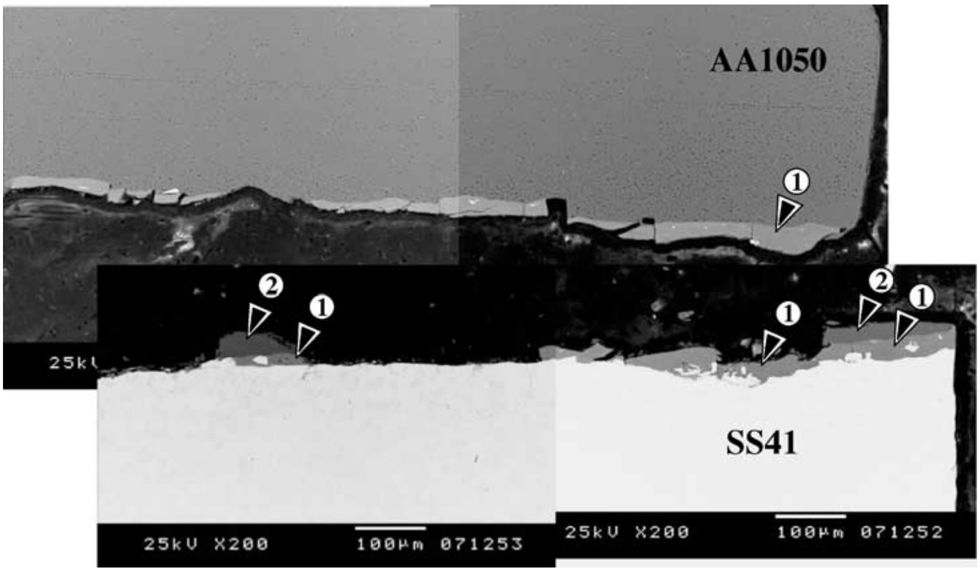

Figure 7 A side view (BE image) of the fractured specimen with 1.0 mm-thick interlayer showing the route of crack propagation. The upper AA1050 part is matched with a lower SS41 steel part at the fracture surface. The right edge of AA1050 part was disappeared after test. The label 1 and 2 are interfacial zone ($FeAl_3$) and AA1050, respectively.

propagation, which is explained in detail in Fig. 9. The specimens with a thicker interlayer have a higher elongation due to plastic deformation of the soft AA1050 aluminum alloy layer. On the other hand, the maximum shear strength decreased with the interlayer thickness. The dependence of the shear deformation properties on the interlayer thickness can be clearly illustrated through the fractography of the fractured surfaces.

Fig. 7 shows a side view (BE image) of the fractured specimen with a 1.0 mm-thick interlayer. The regions labelled 1 and 2 were analyzed as the interfacial zone ($FeAl_3$) and the AA1050, respectively. A line tracing along the fractured surface indicates that cracks propagated through very diverse routes. Most cracks propagated along the interfacial zone/SS41 boundary, and the remaining cracks penetrated the interfacial zone and attacked some local parts of the AA1050 layer just above the AA1050/interfacial zone boundary.

Fig. 8 shows the BE images of the fractured surfaces, in which (a) and (b) are a pair of the fractured surfaces in the specimen with the 0.2 mm-thick interlayer, and (c), (d) and (e) are one side of the fractured surfaces with 0.5, 1.0 and 2.0 mm-thick interlayer, respectively. The BE images of Fig. 8b, c, d and e were taken from the surfaces including the base plate (SS41 plate) of two fractured surfaces. EDS analysis from each fractured surface were carried out parallel with the observation of the fractured surfaces. All the specimens had a similar surface morphology, like a group of islands, except the specimen with the 0.2 mm-thick interlayer. In Fig. 8b, c, d and e, the fractured surfaces generally consisted of two distinct parts, the black part (AA1050) and the gray part (SS41), and their counter surfaces were composed of the AA1050 and the interfacial zone except for the specimen with 0.2 mm-thick interlayer. The specimen with 0.2 mm-thick interlayer showed additionally different features from the thicker specimens. A steel component in the interfacial zone and a wide region of AA5083 were exposed on the fractured surface of the counter part as shown in Fig. 8a.

From the above results, two kinds of schematic diagrams detailing the crack propagation mechanisms with the interlayer thickness are shown in Fig. 9. In the specimen with the thin interlayer (0.2 mm-thick), there were some regions without an interfacial zone, in which the cracks propagated through an other route, such as the AA1050/AA5083 boundary. Therefore, as can be comprehended from the Fig. 8a and b, the crack propagation occurred together at two interfaces, AA5083/AA1050 and interfacial zone/SS41 boundaries, which is in agreement with the reason why the second hardening in Fig. 5 occurs; the AA1050/AA5083 boundary has a higher bond strength than the SS41/interfacial zone boundary. In the specimens with thicker interlayers of 0.5 mm, 1.0 mm, and 2.0 mm, however, the crack propagated through three routes; it split the interfacial zone/SS41 boundary, cut across the interfacial zone, and attacked partially the AA1050 plate just above the AA1050/interfacial zone boundary. Most cracks propagated along the interfacial zone/SS41 boundary. In addition, image analysis from the Fig. 8c, d, and e revealed that the thicker interlayer increases the area fraction of interfacial zone in contact with steel, in the order 45.4%, 50.7%, and 70%, on the fractured surface. This means that the interfacial zone/SS41 boundary is weaker than other interfaces, since the strength decreased with the interlayer thickness, as shown in Fig. 6.

Therefore, it should be considered that the AA1050 aluminum alloy interlayer makes it possible for the welded AA5083/SS41 plates to get good weldability, while generating the interfacial zone between the AA1050 and the SS41 steel plate. The interfacial zone has two detrimental effects on the bond strength; one is to initiate the cracks in the interfacial zone itself and the other is to generate the weak interfacial zone/SS41 boundary. In order to improve the bond strength in explosive welding of an AA5083 aluminum alloy plate and a SS41 steel plate, therefore, a thin interlayer has to be used to minimize the formation of the brittle interfacial zone.

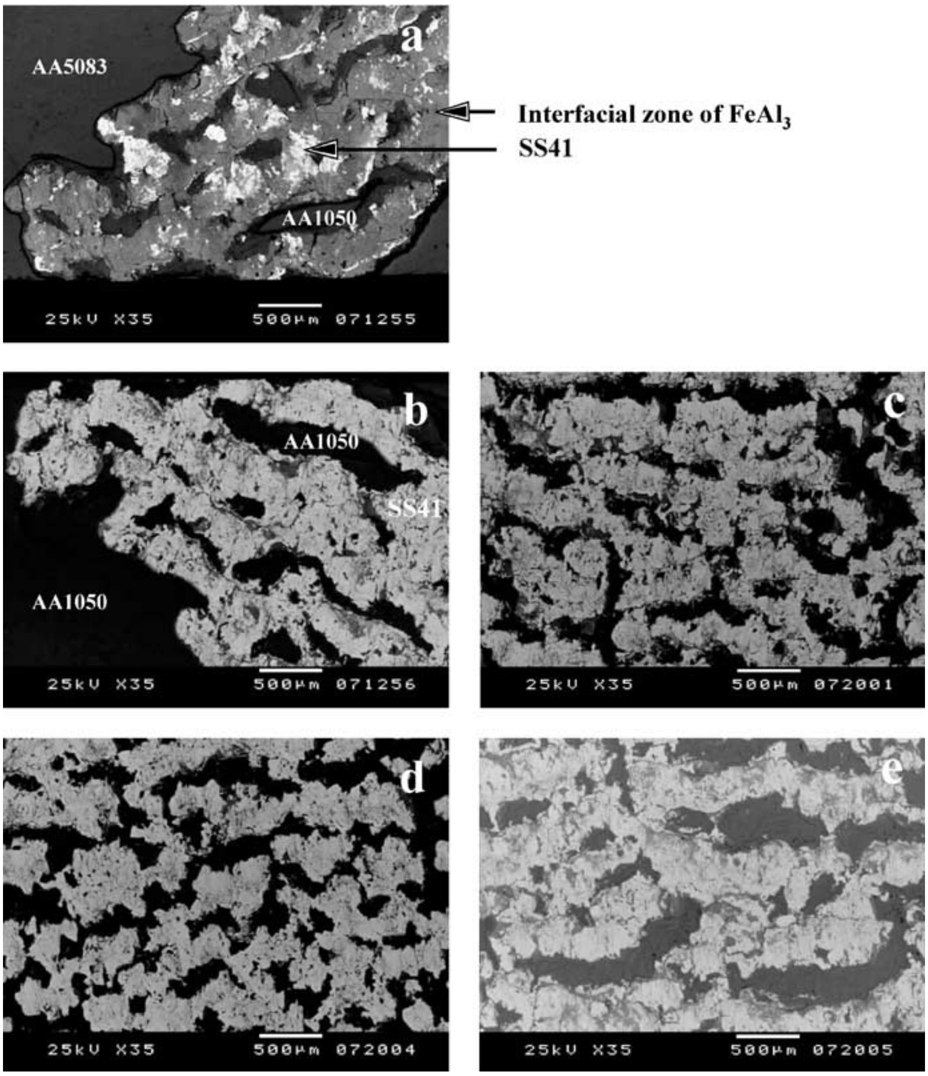

Figure 8 Back scattered electron images of the fractured surfaces, in which (a) and (b) are a pair of the fractured surfaces in the specimen with 0.2 mm-thick interlayer, and (c), (d) and (e) are one side (SS41 part like the Fig. 8b) of the fractured surfaces with 0.5, 1.0 and 2.0 mm-thick interlayer, respectively.

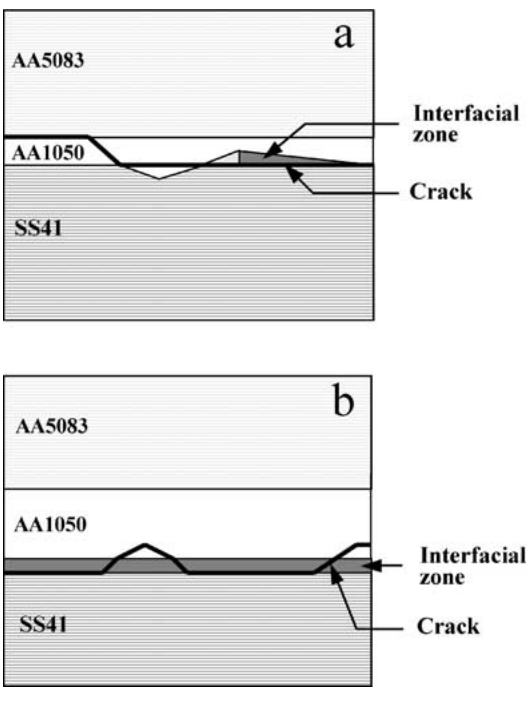

Figure 9 Schematic diagrams about the variations of the crack propagation behavior with the interlayer thickness. (a) thin interlayer (0.2 mm-thick), (b) thicker interlayer (0.5, 1.0, and 2.0 mm-thick).

4. Conclusion

An AA5083 aluminum alloy plate and an SS41 steel plate were cladded by an explosive welding method using an AA1050 aluminum alloy as an interlayer plate. Variations of the interface morphology and the shear deformation behavior depending on the interlayer thickness were investigated.

1. The AA1050 interlayer generated the interfacial zone ($FeAl_3$) which included some cracks in all the specimens. Exceptionally, a discontinuous interfacial zone was formed in the specimen with the 0.2 mm-thick AA1050 interlayer.

2. In the specimen with a thin interlayer (0.2 mm-thick), the crack propagation occurred at the AA5083/AA1050 boundary as well as the interfacial zone/SS41 boundary. Since the AA5083/AA1050 boundary has higher bond strength than the interfacial zone/SS41 boundary, the maximum shear strength of the specimen was higher than in the specimens with the thicker interlayer.

3. In the specimens with a thicker interlayer (0.5 mm, 1.0 mm, and 2.0 mm-thick), most cracks propagated along the weak interface (interfacial zone/SS41

boundary) and the remains of the cracks attacked some inner regions of the AA1050 plate just above the AA1050/interfacial zone boundary. By increasing the thickness of the interlayer, the thickness of the generated interfacial zone increased, and the maximum shear strength gradually decreased, since the area of the weak interfacial zone/SS41 boundary increased.

4. In the case of explosive welding of AA5083 aluminum alloy plate and SS41 steel plate, the thin AA1050 aluminum alloy interlayer plate enhanced the bond strength and suppressed the formation of the brittle interfacial zone.

Acknowledgements
The authors would like to thank to Mr. S. M. Park of Hanwha Co. Ltd. for carrying out explosive welding.

References

1. S. J. KIM, S. H. PAIK and M. Y. HUH, *J. of the Korean Inst. of Met. and Mater.* **32** (1994) 1558.
2. D. G. BRASHER and D. J. BUTLER, *Advanced Materials and Processes* **3** (1995) 37.
3. M. NISHIDA, A. CHIBA, Y. HONDA, J. HIRAZUMI and K. HORIKIRI, *ISIJ International* **35** (1995) 217.
4. S. YANO, H. MATSUI and S. MOROZUMI, *J. Mater. Sci.* **33** (1998) 4857.
5. D. JARAMILLOV, O. T. INAL and A. SZECKET, *ibid.* **22** (1987) 3143.
6. E. S. EGE, O. T. INAL and C. A. ZIMMERLY, *ibid.* **33** (1998) 5327.
7. K. HOKAMOTO, T. IZUMA and M. FUJITA, *Metal. Trans.* **24A** (1993) 2289.

Received 3 April and accepted 9 April 2002